# Feasibility of searches for a Higgs boson using $H \rightarrow W^+W^- \rightarrow l^+l^-$ + missing $p_T$ and high $p_T$ jets at the Fermilab Tevatron

Bruce Mellado, William Quayle, and Sau Lan Wu

*Physics Department, University of Wisconsin-Madison, Madison, Wisconsin 53706, USA*

(Received 19 August 2007; published 21 November 2007)

The sensitivity of standard model Higgs boson searches at the Tevatron experiments with a mass $135 < M_H < 190$ GeV/$c^2$ using the channel $H \rightarrow W^+W^- \rightarrow l^+l^-\not{p}_T (l = e, \mu)$ is discussed. Three new event selections involving Higgs in association with one or two high $P_T$ hadronic jets are discussed. Using leading order matrix elements and a conservative cut-based analysis a 95% confidence level exclusion on $\sigma \times \mathcal{B}(H \rightarrow W^+W^-)$, 1.6 times larger than that predicted by the standard model for $M_H = 165$ GeV/$c^2$, may be achieved with 5 fb$^{-1}$ of integrated luminosity. By combining these three event selections with the existing analysis, the sensitivity of CDF and D0 could improve significantly.

DOI: 10.1103/PhysRevD.76.093007 PACS numbers: 14.80.Bn, 11.30.Qc

## I. INTRODUCTION

In the standard model (SM) of electro-weak and strong interactions, there are four types of gauge vector bosons (gluon, photon, $W^{\pm}$ and $Z$) and 12 types of fermions (six quarks and six leptons) [1–4]. These particles have been observed experimentally. At present, all the data obtained from the many experiments in particle physics are in agreement with the standard model. In the standard model there is one particle, the Higgs boson, that is responsible for giving masses to all of the other particles [5–10]. In this sense, the Higgs particle occupies a unique position.

Before the startup of the Large Hadron Collider (LHC) the Tevatron remains the high energy frontier. The standard model Higgs is expected to be produced predominantly via gluon-gluon fusion [11] and strahlung off a $Z$ or $W^{\pm}$ boson. The third dominant process at the Tevatron is vector boson fusion (VBF) for $M_H \lesssim 200$ GeV/$c^2$ [12,13]. A significant fraction of the Higgs produced via these mechanisms will be associated with at least one high transverse momentum ($P_T$) hadronic jet. The kinematics of Higgs signals in association with jets differ significantly from that of known SM backgrounds.

Searching for a SM Higgs boson at the Tevatron via its decay $H \rightarrow W^+W^-$ was first considered in [14,15]. The relevance of observing a low mass SM Higgs in association with one or two jets of high $P_T$ at the LHC has been pointed out by a number of authors [16–21]. The ATLAS and CMS experiments have confirmed these expectations with detailed detector simulations [22,23]. In this paper we study the sensitivity of the Tevatron experiments to a SM Higgs with a mass $135 < M_H < 190$ GeV/$c^2$ using the decay $H \rightarrow W^+W^- \rightarrow l^+l^-(l = e, \mu)$ in association with hadronic jets. We evaluate the feasibility of three event selection schemes involving events with one or two tagging jets and their impact on the sensitivity to SM Higgs searches for the D0 and CDF experiments.

## II. MC GENERATION OF RELEVANT PROCESSES

For the generation of the Higgs signal processes specified in Sec. I, leading order (LO) matrix elements (ME) were interfaced with the Pythia [24,25] and Herwig [26]. The cross-section computation and the event generation were performed using the parametrization of the parton density functions provided by CTEQ6 [27]. QCD next-to-leading order (NLO) effects are known to be sizeable for the $gg \rightarrow Hj$ process.

The cross sections and kinematics of the Higgs processes were cross-checked with the corresponding ME provided by MCFM [28] and ALPGEN [29]. Table I displays the cross sections for Higgs signal and the main background processes. The cross sections reported in Table I do not take into account the branching fraction of $Z/W^{\pm}$ decays (except for $Z \rightarrow \tau^+\tau^-$) or of any of its decay products. The cross sections of Higgs via gluon-gluon fusion, of $WW$ production and of $Z \rightarrow \tau^+\tau^-$ in association with one jet quoted in Table I, are defined for jet $P_T > 10$ GeV/$c$ and $|\eta| < 100$. The $WW$ process was generated with ALPGEN. The cross sections have been evaluated by setting the renormalization and factorization scales to $\sqrt{M^2 + \sum P_T^2}$ where $M$ is the mass of the weak bosons and the $\sum P_T^2$ stands for the scalar sum of partons in the final state. The cross section for $t\bar{t}$ production used here corresponds to the measured value [30], and the generation was performed with MC@NLO [31,32]. The contribution from processes in which at least one lepton arises from a jet faking a lepton is normalized with respect to the effective cross section of $WW$ + jets. The ratio of the cross section

TABLE I. Cross sections (in fb) of the SM Higgs signal ($M_H = 165$ GeV/$c^2$) and the main background processes considered in this paper (see text).

| $gg \rightarrow Hj$ | $VBFH$ | $VH$ | $WW + 1j$ | $t\bar{t}$ | $Z \rightarrow \tau^+\tau^- + 1j$ |
|---|---|---|---|---|---|
| 96.5 | 37.6 | 61.3 | 3480 | 7200 | 55200 |

 

of fakes to $WW$ + jets is assumed to be the same as in [33]. The contribution from $Z \to l^+l^-$ with $l = e, \mu$ is expected to be negligible due to the requirement of a minimum missing transverse momentum, $\not{p}_T$, a requirement of the minimum transverse momentum of the lepton system and an upper bound on the invariant mass of the two leptons (see Sec. III). The contribution from $Z \to \tau^+\tau^-$, $ZZ$, $ZW^\pm$ and $W^\pm\gamma$ is important. For the sake of simplicity, we assume that the survival probability of processes involving two gauge bosons $ZZ$, $ZW^\pm$, $W^\pm\gamma$ against cuts on jets presented in Sec. III are the same as for $WW$. The contribution from $Z \to \tau^+\tau^-$ + jets was modeled with Pythia using the $2 \to 2$ ME.

In order to emulate detector effects a simple fast simulation program was implemented. Hadrons are clusterized using a classical cone algorithm with $\Delta R < 0.4$. The energy of the resulting hadronic jets was smeared according to a resolution function of the form $\frac{\sigma E}{E} = \frac{a}{\sqrt{E}} \oplus b$. The values of $a$ are set to 0.5, 0.8 for $|\eta| < 0.9$ and $0.9 < |\eta| < 3$, respectively. The values of $b$ are set to 0.03, 0.05 for $|\eta| < 0.9$ and $0.9 < |\eta| < 3$, respectively. The resolution function for electro-magnetic depositions was set to $\frac{\sigma E}{E} = \frac{0.15}{\sqrt{E}} \oplus 0.02$. The reconstructed $\not{p}_T$ follows the following resolution function $\sigma(\not{p}_{x(y)}) = 0.6\sqrt{\sum E_T}$ where $\not{p}_{x(y)}$ is the $x$ ($y$) component of $\not{p}_T$ and $\sum E_T$ is the scalar sum of the transverse energy particles within $|\eta| < 3.5$. Electron and muon identification efficiencies are assumed to be 0.9 in the range $|\eta| < 1.5$ [34]. In the event selection presented in Sec. III D, b-tagging capabilities are used. It is assumed that the b-tagging efficiency is 0.5 for $|\eta| < 1$. In the forward region ($1 < |\eta| < 1.9$) the b-tagging efficiency is parametrized with a linear function $1.05 - 0.55|\eta|$ [34].

## III. EVENT SELECTION

In this section we present the results of three event selections in different corners of the phase space. The three analyses proposed here are orthogonal to one another and relatively good signal-to-background ratios may be achieved. The three event selections presented in Secs. III B, III C, and III D exploit the particular kinematics of the jets in the events produced by the three main signal processes referred to in Sec. I.

### A. Preselection

The final event selections are preceded by a preselection after which the backgrounds are expected to be dominated by $WW$ + jets and $t\bar{t}$ production. The contribution from backgrounds in which one or two leptons arise from misidentification of jets or $b\bar{b}$ events is not expected to be large.

The cuts applied in the preselection are the following: *a)* two opposite sign leptons ($e$, $\mu$) in $|\eta| < 1.5$ with $P_T > 20$ GeV/$c$ for the leading lepton and $P_T > 10$ GeV/$c$ for the subleading one and veto events with a third lepton in $|\eta| < 1.5$ with $P_T > 10$ GeV/$c$; *b)* presence of missing transverse momentum of at least 20 GeV/$c$; *c)* requirement on the invariant mass of the leptons, $20 < M_{ll} < 70$ GeV/$c^2$; *d)* lepton azimuthal angle difference, $\Delta\phi_{ll} < 2.5$ rad, and transverse momentum of the leptonic system, $P_{Tll} > 35$ GeV/$c$.

TABLE II. Effective cross sections (in fb) for signal ($M_H = 165$ GeV/$c^2$) and main background processes after preselection cuts specified in Sec. III A.

| Cut | $gg \to Hj$ | $VBFH$ | $VH$ | $WW + 1j$ | $t\bar{t}$ | $Z \to \tau^+\tau^- + 1j$ |
|---|---|---|---|---|---|---|
| $a$ | 2.50 | 0.97 | 2.73 | 175.95 | 206.02 | 143.22 |
| $b$ | 2.37 | 0.92 | 2.24 | 143.23 | 190.49 | 56.55 |
| $c$ | 1.89 | 0.73 | 1.36 | 69.71 | 49.13 | 54.75 |
| $d$ | 1.68 | 0.64 | 1.14 | 49.96 | 34.84 | 8.19 |

Table II displays the effective cross sections for the three signal processes and backgrounds for cuts $a$–$c$. It is relevant to note that no requirement on the presence of jets has been made in Table II. The requirements on the minimum $\not{p}_T$ and the invariant mass of the two leptons in cuts $c$ and $d$ enhances the ratio of signal to the main backgrounds by about a factor of 2. These cuts diminish the discriminating power of variables such as the transverse mass of the leptons and the $\not{p}_T$ or the azimuthal angle difference between the two leptons. The requirements applied in cut $d$ are mainly intended to suppress the Drell-Yan process $Z \to \tau^+\tau^- \to l^+l^-\not{p}_T$. The presence of $\not{p}_T$ is a strong discriminator against this process. However, in events with jets studied here a cut on $\not{p}_T$ is not enough to achieve the necessary rejection. The requirement on the minimum transverse momentum of the lepton pair is particularly effective in reducing Drell-Yan backgrounds.

### B. Selection I

The selection proposed here takes advantage of the fact that the leading jet produced in association with Higgs via the gluon-gluon fusion and the VBF processes tends to be more forward than in background events, as illustrated in Fig. 1. Figure 1 displays the pseudorapidity distribution of the leading jet in the event for signal and background processes after the application of the preselection requirements given in Sec. III A.

Because of the potential contribution from the Higgs signal produced via VBF it is important to reconstruct jets to the very forward region. Therefore in this selection we assume the ability to reconstruct jets of $P_T > 15$ GeV/$c$ in the range $|\eta| < 3$.

The event selection is comprised of the following cuts: *Ia)* at least one jet with $P_T > 15$ GeV/$c$ in the range $|\eta| < 3$; *Ib)* if the event has at least two jets with $P_T > 15$ GeV/$c$ in the range $|\eta| < 3$ it is required that the event fails the two-jet event selections presented in Secs. III C and III D; *Ic)* if a second jet is found with $P_T > 15$ GeV/$c$ and

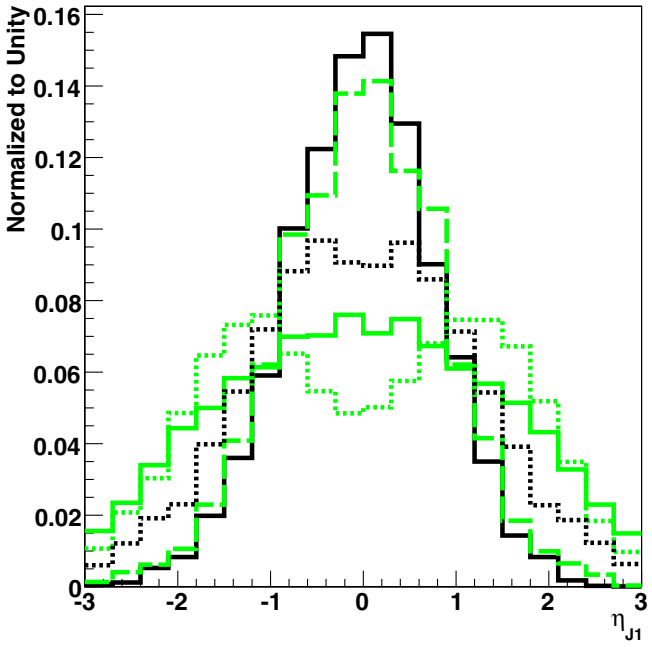


FIG. 1 (color online). The pseudorapidity of the leading jet for signal and background processes after the application of preselection cuts presented in Sec. III A. The solid, dotted and dashed light-colored histograms correspond to gluon-gluon fusion, VBF and $VH$ signal production, respectively. The solid and dotted black histograms correspond to $t\bar{t}$ and $WW$ + jets, respectively.

$|\eta| < 1.25$ the event is rejected; *Id)* require that the leading jet be relatively forward, $1.25 < |\eta| < 3$.

Table III displays the effective cross section for signal and background processes after the application of the preselection cuts in Sec. III A and the above cuts. Cut *Ib* is introduced to avoid double counting of events passing selections presented in Secs. III C and III D. Cut *Ic* is introduced instead of a full jet veto in the entire range $|\eta| < 3$ in order to enhance the contribution from Higgs signal events produced by the VBF mechanism. These types of events evolve from a residual fraction of events that do not pass the stringent two-jet event selection presented in Sec. III C, specifically the requirement that the pseudorapidity difference between the jets be greater than a large value. A significant fraction of Higgs events produced via the $VH$ mechanism are lost after cut *Ic*. In order to recover these events a third event selection is presented here (see Sec. III D).

Because of the application of cuts *Ic–Id* the two leading jets in the event tend to be in a pseudorapidity range in which the b-tagging efficiency is rather small. Therefore the b-tagging capability was not used to further suppress $t\bar{t}$ background.

The rows after cut *Id* in Table III correspond to tighter cuts on the pseudorapidity of the leading jets. By tightening the requirement on the "forwardness" of the leading jet the signal-to-background ratio improves significantly with respect to cut *Id*. As far as the sensitivity is concerned, the optimal value of the range of the pseudorapidity of the leading jet is $1.25 < |\eta| < 3$.

### C. Selection II

The event selection presented here is tuned to enhance the Higgs contribution from the VBF mechanism. Figure 2 shows the distributions of the rapidity gap between the two leading jets, $\Delta\eta_{jj}$, for signal and background processes. It is important to note that the distribution for the VBF signal process shown in Fig. 2 enhances the fraction of the events with a small $\eta$ separation with respect to the one predicted by the fixed order NLO computation by MCFM. The corresponding distribution for the signal process via gluon-gluon fusion, although it is expected to be small, is not reliable since in the MC generation used here no ME correction was applied on the subleading jet.

The rate and angular distributions of additional jet activity with $P_T > 15$ GeV$/c$ were investigated in signal and background processes. This is motivated by the fact that the leading signal contribution comes from a color singlet exchange and a reduced rate of hadronic jets is expected in the signal-like region. A veto on additional jet activity was found to give additional discriminating power against $t\bar{t}$ production, but was not used here. Further investigation could be performed by lowering the $P_T$ threshold to 10 GeV$/c$.

The event selection comprises the following cuts: *IIa)* at least two jets with $P_T > 15$ GeV$/c$ in the range $|\eta| < 3$; *IIb)* large difference in pseudorapidity between the two leading jets, $\Delta\eta_{jj} > 2.5$.

Table IV displays the effective cross sections for signal as well as backgrounds and the signal-to-background ratios

TABLE III. Effective cross sections (in fb) for signal and background processes after selection cuts specified in Sec. III B. The last column shows the resulting signal-to-background ratio.

| Cut | $gg \to Hj$ | $VBFH$ | $VH$ | $WW$ | $t\bar{t}$ | $Z \to \tau^+\tau^-$ | Other | S/B |
|---|---|---|---|---|---|---|---|---|
| *Ia* | 0.95 | 0.60 | 0.97 | 11.51 | 34.52 | 8.14 | 6.26 | 0.04 |
| *Ib* | 0.85 | 0.46 | 0.52 | 10.82 | 25.96 | 7.50 | 5.89 | 0.04 |
| *Ic* | 0.74 | 0.34 | 0.36 | 9.57 | 9.28 | 6.25 | 5.25 | 0.05 |
| *Id* | 0.33 | 0.16 | 0.07 | 2.86 | 1.17 | 1.05 | 1.61 | 0.08 |
| $\|\eta_j\| > 1.5$ | 0.26 | 0.12 | 0.04 | 1.99 | 0.71 | 0.55 | 1.14 | 0.10 |
| $\|\eta_j\| > 1.75$ | 0.19 | 0.08 | 0.02 | 1.33 | 0.36 | 0.28 | 0.78 | 0.11 |

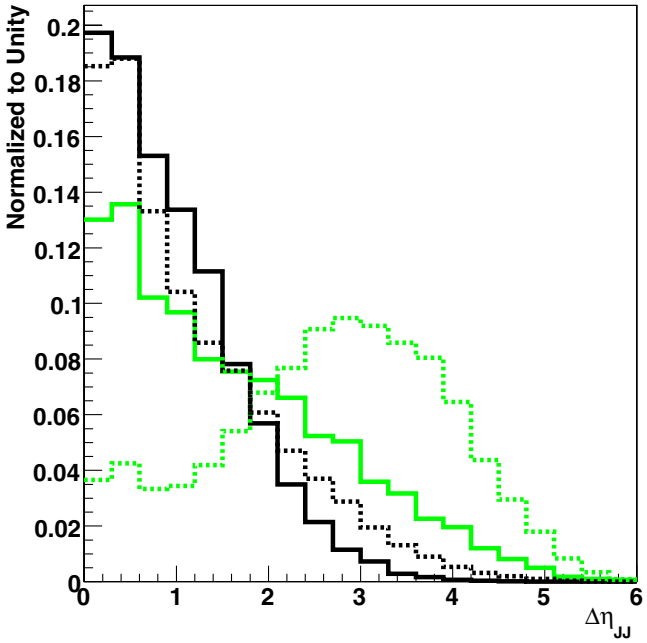


FIG. 2 (color online). The pseudorapidity difference of the two leading jets for signal and background processes after the application of preselection cuts presented in Sec. III A. The solid and dotted light-colored histograms correspond to gluon-gluon fusion and VBF signal production, respectively. The solid and dotted black histograms correspond to $t\bar{t}$ and $WW$ + jets, respectively.

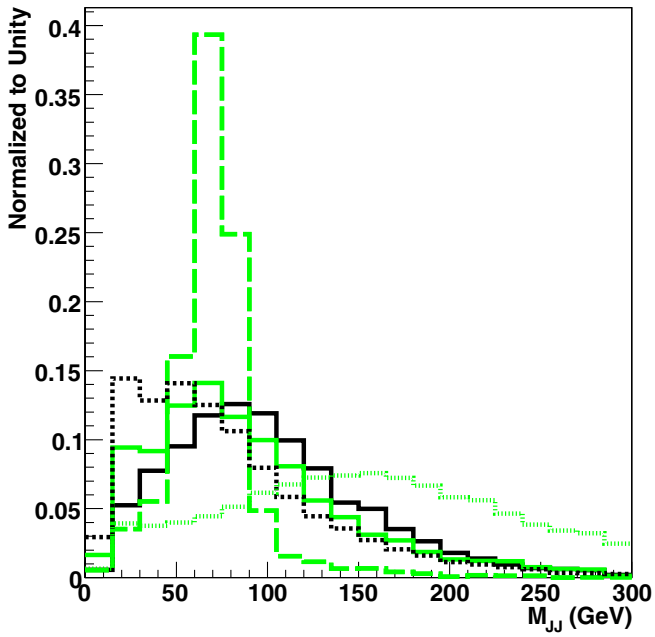


FIG. 3 (color online). The invariant mass of the two leading jets after the application of preselection cuts presented in Sec. III A. The solid, dotted and dashed light-colored histograms correspond to gluon-gluon fusion, VBF and $VH$ signal production, respectively. The solid and dotted black histograms correspond to $t\bar{t}$ and $WW$ + jets, respectively.

after the application of cuts *IIa–IIb*. The last four rows in Table IV correspond to the application of tighter cuts on $\Delta\eta_{jj}$. The optimal value on the cut on the di-jet pseudorapidity difference to achieve the best 95% confidence limit is $\Delta\eta_{jj} > 3$.

### D. Selection III

The event selection proposed here is intended to enhance the efficiency of tagging $VH$ with $V \to qq'$. This is mostly achieved by requiring that the invariant mass of the two leading jets be close to the mass of the $Z$, $W$ bosons. Figure 3 displays the invariant mass of the two leading jets for signal and background processes after the application of the preselection requirements given in Sec. III A.

The event selection is composed of the following cuts: *IIIa)* at least two jets with $P_T > 20$ GeV/$c$ in the range $|\eta| < 2.5$; *IIIb)* it is required that the event does not pass the selection presented in Secs. III C; *IIIc)* b-jet veto selection (see Sec. II); *IIId)* invariant mass of the two leading jets, $50 < M_{jj} < 80$ GeV/$c^2$.

Table V shows the effective cross sections for signal as well as backgrounds and the signal-to-background ratios after the application of cuts *IIIa–IIId*. After the application of cuts *IIIa–IIIc* the $t\bar{t}$ process becomes the dominant one. As the two leading jets in this selection are central, the ability to tag $b$-jets becomes essential. The enhancement of $b$-tagging efficiency is, however, not the only handle to further suppress the $t\bar{t}$ background.

## IV. RESULTS AND CONCLUSIONS

The event selections presented in Secs. III B, III C, and III D were optimized for $M_H = 165$ GeV/$c^2$ and no further mass dependent optimization was implemented.

TABLE IV. Effective cross-sections (in fb) for signal and background processes after selection cuts specified in Sec. III C. The last column shows the resulting signal-to-background ratio.

| Cut | $gg \to Hj$ | $VBFH$ | $VH$ | $WW$ | $t\bar{t}$ | $Z \to \tau^+\tau^-$ | Other | S/B |
|---|---|---|---|---|---|---|---|---|
| *IIa* | 0.28 | 0.41 | 0.66 | 2.50 | 29.62 | 2.66 | 1.31 | 0.04 |
| *IIb* | 0.06 | 0.24 | 0.01 | 0.27 | 1.14 | 0.34 | 0.14 | 0.16 |
| $\Delta\eta_{jj} > 3.0$ | 0.04 | 0.17 | 0.00 | 0.13 | 0.39 | 0.17 | 0.07 | 0.29 |
| $\Delta\eta_{jj} > 3.5$ | 0.02 | 0.11 | 0.00 | 0.06 | 0.11 | 0.07 | 0.04 | 0.49 |
| $\Delta\eta_{jj} > 4.0$ | 0.01 | 0.06 | 0.00 | 0.03 | 0.03 | 0.02 | 0.01 | 0.80 |

TABLE V. Effective cross sections (in fb) for signal and background processes after selection cuts specified in Sec. III D. The last column shows the resulting signal-to-background ratio.

| Cut | $gg \to Hj$ | $VBFH$ | $VH$ | $WW$ | $t\bar{t}$ | $Z \to \tau^+\tau^-$ | Other | S/B |
|---|---|---|---|---|---|---|---|---|
| *IIIa* | 0.16 | 0.30 | 0.53 | 1.54 | 26.79 | 1.89 | 0.80 | 0.03 |
| *IIIb* | 0.15 | 0.20 | 0.53 | 1.49 | 26.57 | 1.82 | 0.77 | 0.03 |
| *IIIc* | 0.14 | 0.20 | 0.51 | 1.47 | 9.94 | 1.80 | 0.76 | 0.06 |
| *IIId* | 0.05 | 0.02 | 0.37 | 0.43 | 2.68 | 0.39 | 0.23 | 0.12 |

TABLE VI. Expected 95% confidence level limit expressed in terms of the ratio of $\sigma \times \mathcal{B}$ over the corresponding value in the standard model. Results are given as a function of the Higgs mass (in GeV/$c^2$) with 5 fb$^{-1}$ and 10 fb$^{-1}$ of integrated luminosity for two experiments combined.

| $M_H$ | 135 | 140 | 145 | 150 | 155 | 160 | 165 | 170 | 175 | 180 | 185 | 190 | 195 |
|---|---|---|---|---|---|---|---|---|---|---|---|---|---|
| 5 fb$^{-1}$ | 3.2 | 2.7 | 2.3 | 2.1 | 1.9 | 1.7 | 1.6 | 1.8 | 2.0 | 2.3 | 2.9 | 3.5 | 4 |
| 10 fb$^{-1}$ | 2.1 | 1.7 | 1.5 | 1.4 | 1.2 | 1.1 | 1.1 | 1.2 | 1.3 | 1.5 | 1.9 | 2.3 | 2.7 |

Therefore, when evaluating sensitivity the background contribution remains unchanged for different Higgs mass hypotheses. A mass optimization is expected to yield additional sensitivity, especially for Higgs masses $M_H < 150$ GeV/$c^2$ where discriminants such as the scalar sum of the leptons and $\not{p}_T$ of the transverse mass of the lepton-neutrino system yield separation against $WW$ and $t\bar{t}$ processes. For Higgs masses $M_H > 170$ GeV/$c^2$ the relaxation of the upper bound of the leptonic invariant mass can enhance the signal contribution while maintaining the signal-to-background ratio.

The expected exclusion limit was calculated using a likelihood technique [35,36]. Table VI shows the expected 95% confidence level limit as a function of the Higgs mass with 5 fb$^{-1}$ and 10 fb$^{-1}$ of integrated luminosity (for two experiments combined).

In conclusion, the searches of a Higgs boson using $W^+W^- +$ jets with the event selections presented in this paper could further enhance the sensitivity of the Tevatron experiments reported in [33,37,38]. It is important to note that we use LO cross sections for the $gg \to Hj$ process. The NLO K-factors for this process are expected to be large, thus significantly enhancing the sensitivity of analysis *I*. In addition, no multivariate techniques have been implemented. With the tagging of hadronic jets the complexity of the final state increases and with it the relative sensitivity of a multivariate analysis with respect to the simple cut-based approach used here. In particular, variables like the transverse mass of the Higgs-leading jet system and the invariant mass of the two leading jets can be used as additional discriminating variables when appropriate. The analysis strategy presented here is conservative and leaves room for significant improvement.

## ACKNOWLEDGMENTS

The authors are most grateful to Y. Fang, L. Flores-Castillo, T. Han, M. Herndon, F. Petriello and T. Vickey for most valuable comments and suggestions. This work was supported in part by the United States Department of Energy through Grant No. DE-FG0295-ER40896.

[1] S. L. Glashow, Nucl. Phys. **22**, 579 (1961).
[2] S. Weinberg, Phys. Rev. Lett. **19**, 1264 (1967).
[3] A. Salam, in *Proceedings to the Eighth Nobel Symposium, May 1968*, edited by N. Svartholm (Wiley, New York, 1968), p. 357.
[4] S. L. Glashow, J. Iliopoulos, and L. Maiani, Phys. Rev. D **2**, 1285 (1970).
[5] F. Englert and R. Brout, Phys. Rev. Lett. **13**, 321 (1964).
[6] P. W. Higgs, Phys. Lett. **12**, 132 (1964).
[7] P. W. Higgs, Phys. Rev. Lett. **13**, 508 (1964).
[8] P. W. Higgs, Phys. Rev. **145**, 1156 (1966).
[9] G. S. Guralnik, C. R. Hagen, and T. W. B. Kibble, Phys. Rev. Lett. **13**, 585 (1964).
[10] T. W. B. Kibble, Phys. Rev. **155**, 1554 (1967).
[11] H. M. Georgi, S. L. Glashow, M. E. Machacek, and D. V. Nanopoulos, Phys. Rev. Lett. **40**, 692 (1978).
[12] R. Cahn and S. Dawson, Phys. Lett. B **136**, 196 (1984).
[13] G. Kane, W. Repko, and W. Rolnick, Phys. Lett. B **148**, 367 (1984).
[14] T. Han and R.-J. Zhang, Phys. Rev. Lett. **82**, 25 (1999).
[15] T. Han, A. S. Turcot, and R.-J. Zhang, Phys. Rev. D **59**, 093001 (1999).

[16] D. L. Rainwater and D. Zeppenfeld, J. High Energy Phys. 12 (1997) 5.
[17] D. L. Rainwater and D. Zeppenfeld, Phys. Rev. D **60**, 113004 (1999).
[18] D. L. Rainwater, D. Zeppenfeld, and K. Hagiwara, Phys. Rev. D **59**, 014037 (1998).
[19] T. Plehn, D. L. Rainwater, and D. Zeppenfeld, Phys. Rev. D **61**, 093005 (2000).
[20] S. Abdullin *et al.*, Phys. Lett. B **431**, 410 (1998).
[21] B. Mellado, W. Quayle, and Sau Lan Wu, Phys. Lett. B **611**, 60 (2005).
[22] S. Asai *et al.*, Eur. Phys. J. C **32**, s19 (2004).
[23] CMS Collaboration, CMS PTDR V.2: Physics Performance, Report No. CERN/LHCC 2006-021.
[24] T. Sjöstrand, Comput. Phys. Commun. **82**, 74 (1994).
[25] T. Sjöstrand *et al.*, Comput. Phys. Commun. **135**, 238 (2001).
[26] G. Corcella *et al.*, J. High Energy Phys. 01 (2001) 010.
[27] J. Pumplin *et al.*, J. High Energy Phys. 07 (2002) 012.
[28] J. M. Campbell and R. K. Ellis, Phys. Rev. D **62**, 114012 (2000)
[29] M. L. Mangano *et al.*, J. High Energy Phys. 07 (2003) 001.
[30] CDF Collaboration, CDF Note 8148.
[31] S. Frixione and B. R. Webber, J. High Energy Phys. 06 (2002) 029.
[32] S. Frixione and B. R. Webber, J. High Energy Phys. 08 (2003) 007.
[33] CDF Collaboration, CDF Note 8774.
[34] M. Herndon (private communication).
[35] K. Cranmer, B. Mellado, W. Quayle, and Sau Lan Wu, ATLAS Note ATL-PHYS-2003-008, 2003.
[36] K. Cranmer, B. Mellado, W. Quayle, and Sau Lan Wu, arXiv:physics/0312050.
[37] D0 Collaboration, Conference Note 5194-CONF.
[38] D0 Collaboration, Conference Note 5332-CONF.